

1 *Type of the Paper (Article, Review, Communication, etc.)*

## 2 **Non-dispersive extraction of Ge(IV) from aqueous** 3 **solutions by Cyanex 923: Transport and modeling** 4 **studies**

5 **Hossein Kamran Haghighi**<sup>1</sup>, **Mehdi Irannajad**<sup>1,\*</sup>, **Maria Teresa Coll**<sup>2</sup> and **Ana Maria Sastre**<sup>3</sup>

6 <sup>1</sup> Department of Mining and Metallurgy, Amirkabir University of Technology, Tehran, Iran;

7 [h.kamran.h@aut.ac.ir](mailto:h.kamran.h@aut.ac.ir); [irannajad@aut.ac.ir](mailto:irannajad@aut.ac.ir)

8 <sup>2</sup> Department of Chemical Engineering, Universitat Politècnica de Catalunya, EPSEVG, Av. Víctor Balaguer  
9 s/n, 08800 Vilanova i la Geltrú, Spain.; [m.teresa.collupc.edu](mailto:m.teresa.collupc.edu)

10 <sup>3</sup> Department of Chemical Engineering, Universitat Politècnica de Catalunya, ESTEIB, Av. Diagonal 647,  
11 08028 Barcelona, Spain; [ana.maria.sastre@upc.edu](mailto:ana.maria.sastre@upc.edu)

12

13 **Abstract:** The transport of germanium from an aqueous solution containing oxalic acid was studied  
14 using a flat sheet supported liquid membrane (FSSLM) system. Cyanex 923 immobilized in a  
15 polytetrafluoroethylene membrane was employed as a carrier. The solution chemistry and related  
16 diagrams were applied to study the transport of germanium. The effectual parameters such as  
17 oxalic acid, the carrier, and strip reagent concentrations were evaluated in this study. Based on the  
18 results, the oxalic acid concentration of 0.075 mol/L and the carrier concentration of 20 %v/v were  
19 the condition in which the efficient germanium transport occurred. Among strip reagents tested,  
20 NaOH had the best efficiency to transport germanium through the supported liquid membrane  
21 system. Furthermore, the permeation model was obtained to calculate the mass transfer resistances.  
22 According to the results, the values of 1 and 1345 s/cm were evaluated for  $\Delta m$  and  $\Delta f$ , respectively.  
23 The model curve showed that the P value reached a steady state at higher concentrations of the  
24 carrier because the viscosity governed the transport phenomenon.

25 **Keywords:** Germanium; Supported liquid membrane; Transport; Cyanex 923; Modeling

26

### 27 **1. Introduction**

28 Germanium is a strategic metalloid applied to a wide range of high-technology devices [1].  
29 Germanium is found in lead and zinc ores [2] and fly ashes from coals [3]. From the view of  
30 hydrometallurgy, the leach solutions obtained from the zinc plant residues and coal fly ashes  
31 contain germanium along with other metals. The most important elements that can be found in these  
32 solutions are heavy metals such as zinc, nickel, cobalt, etc. [4,5]. The germanium separation from  
33 these solutions is a vital objective to obtain a purified germanium product.

34 Gasification coal fly ashes containing germanium can be leached with water to dissolve  
35 germanium as water-soluble species [6]. Several processes have been developed to recover and  
36 separate germanium from impurities such as precipitation [7], flotation [8], ion-exchange [9],  
37 distillation [3], adsorption [10], and liquid-liquid extraction (LLX) [11]. Among these techniques, the  
38 LLX processes have been extensively applied to separate germanium from aqueous solutions [12].  
39 However, some disadvantages make this method inappropriate for treating low concentrations of  
40 ions. The supported liquid membrane (SLM) techniques have been introduced as alternative  
41 methods to overcome these disadvantages [13]. High selectivity, user-friendly operation, low  
42 consumption of carrier, and the one-step process are some advantages of SLMs [14-17].

43 Cyanex 923 is an extractant with solvation extraction behavior containing four trialkyl  
44 phosphine oxides, which can be used to extract neutral species. This extractant has been widely used  
45 in SLM systems. The permeation of cadmium ( $H(n-2)CdCl_n$ ) from wastewater containing chloride

46 anions has been investigated through SLM processes using Cyanex 923 [18]. Chromium(VI) neutral  
47 species ( $\text{H}_2\text{CrO}_4$ ) was transported across an FSSLM system using Cyanex 923 from chloride  
48 solutions [19]. Zinc(II) species in the form of  $\text{HnZnCl}_{(2+n)}$  were permeated by a solid-SLM from  
49 chloride medium using Cyanex 923 [20]. In addition, an FSSLM system has been used to transport  
50  $\text{HFeCl}_4$  species through a PVDF membrane with the carrier of Cyanex 923 from a solution  
51 containing chloride ions [21]. Alguacil, *et al.* [22] investigated the transport of Au(III) in the form  
52  $\text{HAuCl}_4$  through a PVDF membrane film impregnated in Cyanex 923 from HCl solution. Results  
53 showed good transport efficiency for gold species. Neutral complexes of uranium(VI)  
54 ( $\text{UO}_2(\text{H}_2\text{PO}_4)_2$ ) were separated through an SLM system from phosphoric acid solutions using  
55 mobile carriers containing 2-ethyl hexyl phosphoric acidmono-2-ethyl hexyl ester (PC88A) and  
56 Cyanex 923 [23].

57 The presented research describes a flat-sheet supported liquid membrane (FSSLM) process with  
58 a Cyanex 923 carrier, in which the facilitated transport of germanium species is carried out from a  
59 solution containing oxalic acid. Significant parameters affecting the transport of germanium such as  
60 germanium concentration in the feed phase, carrier concentration, oxalic acid concentration,  
61 membrane type, and NaOH concentration in the strip phase have been investigated in detail.  
62 Finally, a mass transfer model was developed to find the  $\Delta a_q$  and  $\Delta \text{org}$  values, which are resistances  
63 corresponding to the species diffusion through the feed-membrane interfacial layer and membrane  
64 phase, respectively.

## 65 2. Experimental

### 66 2.1. Materials

67 Cyanex 923 consisting of four trialkyl phosphine oxides (93%) was supplied by CYTEC Inc., NJ,  
68 USA. Various concentrations of the mobile carrier (5-30 %v/v) were prepared by dissolving Cyanex  
69 923 in kerosene (Sigma-Aldrich, MO, USA). In all experiments, purified water was used supplied  
70 using a water purifier (Siemens, Germany). The solution used in this study was a solution containing  
71 100 mg/L of germanium prepared by dissolving  $\text{GeO}_2$  (99.99%) provided by Sigma-Aldrich. Desired  
72 amounts of oxalic acid powder from Panreac, Barcelona, Spain were added to the aforementioned  
73 solutions to prepare various oxalate concentrations in the range of 0.05-0.2 mol/L. In order to choose  
74 a proper stripping phase, some reagents provided by Sigma-Aldrich such as ammonium chloride  
75 ( $\text{NH}_4\text{Cl}$ ), sodium hydroxide (NaOH), catechol ( $\text{C}_6\text{H}_6\text{O}_2$ ), citric acid ( $\text{C}_6\text{H}_8\text{O}_7$ ), ammonia ( $\text{NH}_3$ ),  
76 sodium sulfate ( $\text{Na}_2\text{SO}_4$ ), sulfuric acid ( $\text{H}_2\text{SO}_4$ ) and purified water were used as stripping phases.

77 A FHLP series of poly tetra fluoro ethylene (PTFE) flat sheet hydrophobic membranes with the  
78 characteristics being a porosity of 85%, 47 mm diameter, and pore size of 0.45  $\mu\text{m}$  and a HVHP series  
79 of polyvinylidene difluoride (PVDF) hydrophobic membrane with a pore size of 0.45 $\mu\text{m}$ , diameter  
80 of 47 mm, and thickness of 125  $\mu\text{m}$  were supplied from Millipore, KGaA, Darmstadt, Germany.

### 81 2.2. Membrane experiments

82 FSSLM experiments were carried out in a system including two cells attached together with a  
83 flanged chamber between the cells in which a membrane filter could be placed. The effective  
84 membrane area was calculated to be 11  $\text{cm}^2$ . The configuration of this system was introduced  
85 elsewhere [24]. The system contained two cells for the feed and strip (receiving) phases with a  
86 volume of 220 mL for each cell. Before starting the experiments, the membranes were impregnated  
87 in various concentrations of Cyanex 923 diluted in kerosene. The feed and strip phases were mixed  
88 well by means of a mechanical stirrer. Samples with volumes of 0.5 mL from both phases were taken  
89 to evaluate the concentrations of ions during the experiments. The composition of solutions was  
90 determined using an inductively coupled plasma atomic emission spectroscopy (ICP-AES Agilent,  
91 USA).

92  
93

### 94 2.3. Transport equations

95 Transport phenomena in SLM processes principally occur in three steps including the reaction  
96 of species with the carrier at the feed-membrane interface, diffusion across the membrane and  
97 stripping at the membrane-strip interface. According to the literature, the flux of species (J) can be  
98 found by disregarding the concentration of germanium in the strip phase with respect to Eq. (1) [14]:

$$99 \quad J = P_f C_f \quad (1)$$

100 In this equation,  $P_f$  represents the permeability coefficient at the feed-membrane interface and  
101  $C_f$  depicts the ions concentration in the feed phase. Furthermore, the flux can be written according to  
102 Fick's first law in a differential form as Eq. (2):

$$103 \quad J = -\frac{V}{A} \left( \frac{dC_f}{dt} \right) \quad (2)$$

104 Where  $V$  is the volume of the feed phase and  $A$  shows the membrane efficient area. With  
105 respect to Eqs. (1) and (2), the integration form of Eq. (2) and Eq. (3) can be written as:

$$106 \quad \ln(C_{f,0} / C_{f,t}) = -\frac{AP_f t}{V} \quad (3)$$

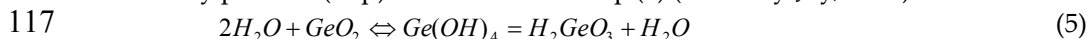
107 Where  $C_{f,0}$  and  $C_{f,t}$  depict the concentration of ions in the feed phase at the initial time and  
108 time of ' $t$ ', respectively. Hence, the permeability coefficient can be evaluated from the slope  
109 corresponding to the plot of  $\ln(C_{f,0} / C_{f,t})$  against  $-\frac{At}{V}$ . Furthermore, the transport efficiency  
110 (%Transport) of germanium is calculated as Eq. (4):

$$111 \quad \%T = \frac{C_{f,t}}{C_{f,0}} \times 100 \quad (4)$$

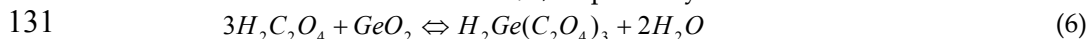
112

### 113 3. Solution chemistry

114 Germanium dioxide can be dissolved in water. However, this dissolution is slowly carried out  
115 as an intermediate tetra-hydroxide. These species can be converted to Germanic acid with the  
116 solubility product ( $K_{sp}$ ) of  $2.39 \times 10^{-4.5}$  as Eq. (5) (McCrorry-Joy, 1985):



118 Germanium can form various complexes with organic acid such as tartaric acid, citric acid,  
119 oxalic acid, etc. Oxalic acid is a possible complexant, forming various complexes with germanium.  
120 Furthermore, it can form similar complexes with other metals. According to the literature and  
121 observations, the solubility of germanium increases in the presence of oxalic acid in aqueous  
122 solutions (Liu et al., 2017b). The formation of germanium anionic and neutral species has been  
123 reported. For instance, Pokrovski et al. (2000) described that germanium (0.02 mol/L) and oxalic acid  
124 (0.1 mol/L) form anionic species of  $Ge(OH)_2(ox)_2^{2-}$  ("ox" depicts oxalate) at pHs below 7.  
125 Furthermore, in a research conducted by Liu et al. (2017a)  $Ge(ox)_3^{2-}$  was introduced as anionic  
126 complexes of germanium and oxalic acid extracted by tri(octyl-decyl) amine (N235). The  
127 concentrations of germanium and oxalic acid in the latter study were reported to be 0.013 and 0.67  
128 mol/L, respectively. However, others (Kamran Haghghi et al., 2018; McCrorry-Joy, 1985) reported  
129 the formation of neutral species of trisoxalato germanates as Eq. (6), as germanium and oxalic acid  
130 concentrations were 0.11 and 1 mol/L, respectively:



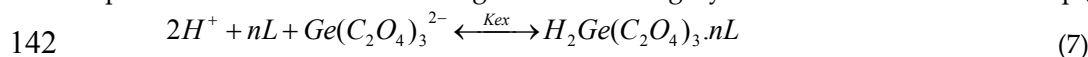
132 In the current study, since germanium could be extracted and transported by Cyanex 923,  
133 having the solvation mechanism, it can be concluded that germanium neutral soluble species in the  
134 form of trisoxalato germanate have been extracted by the carrier.

135 This section may be divided by subheadings. It should provide a concise and precise  
136 description of the experimental results, their interpretation as well as the experimental conclusions  
137 that can be drawn.

## 138 4. Results and discussions

### 139 4.1. Determination of the extraction mechanism by slope analysis

140 With respect to the "solution chemistry" section and the literature review [18,25,26], the  
141 probable extraction reaction of germanium using Cyanex 923 can be written as Eq. (7):



143 Where L depicts the organic extractant (Cyanex 923) and K<sub>ex</sub> shows the equilibrium constant.  
144 In order to find the number of extractant molecules that participated in the reaction, a series of  
145 liquid-liquid extraction experiments was conducted. According to Eq. (7), K<sub>ex</sub> can be written as Eq.  
146 (8):

$$147 \quad K_{ex} = \frac{[H_2Ge(C_2O_4)_3 \cdot nL]}{[H^+]^2 [L]^n [Ge(C_2O_4)_3^{2-}]} \quad (8)$$

148 Since  $\frac{[H_2Ge(C_2O_4)_3 \cdot nL]}{[Ge(C_2O_4)_3^{2-}]}$  is equal to the distribution coefficient (D) at an equilibrium state, Eq. (8)  
149 can be written as Eq. (9):

$$150 \quad K_{ex} = \frac{D}{[H^+]^2 [L]^n} \quad (9)$$

151 By taking the logarithm of Eq. (9), Eq. (10) was rearranged:

$$152 \quad \log(D) = \log K_{ex} + 2 \log[H^+] + n \log[L] \quad (10)$$

153 The plot of the distribution coefficient (D) as a function of the extractant concentration was  
154 constructed to determine the number of Cyanex 923 molecules that reacted with transported  
155 germanium species. The obtained plot is illustrated in Figure 1. As seen in this figure, the slope of the  
156 linearized plot was found to be 3.60. Hence, it was concluded that 4 molecules of Cyanex 923 were  
157 associated with germanium species.

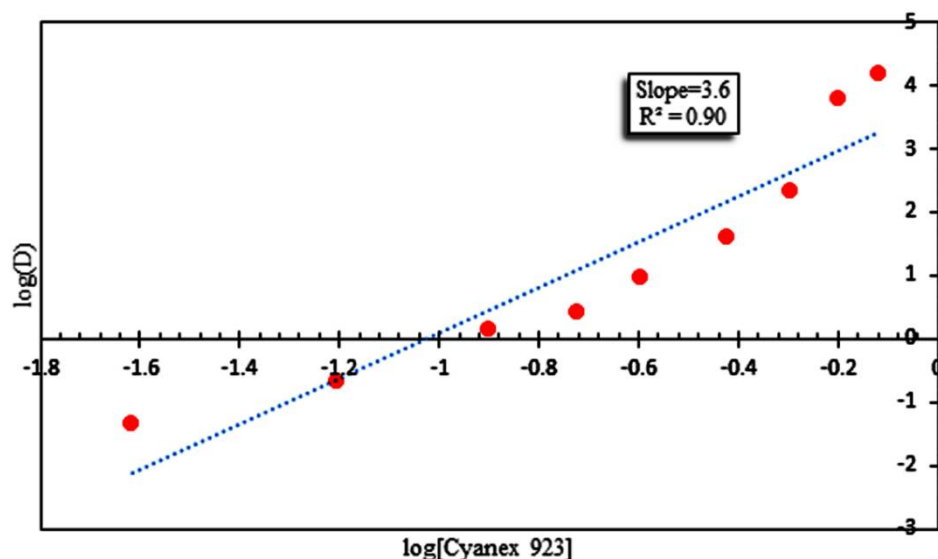
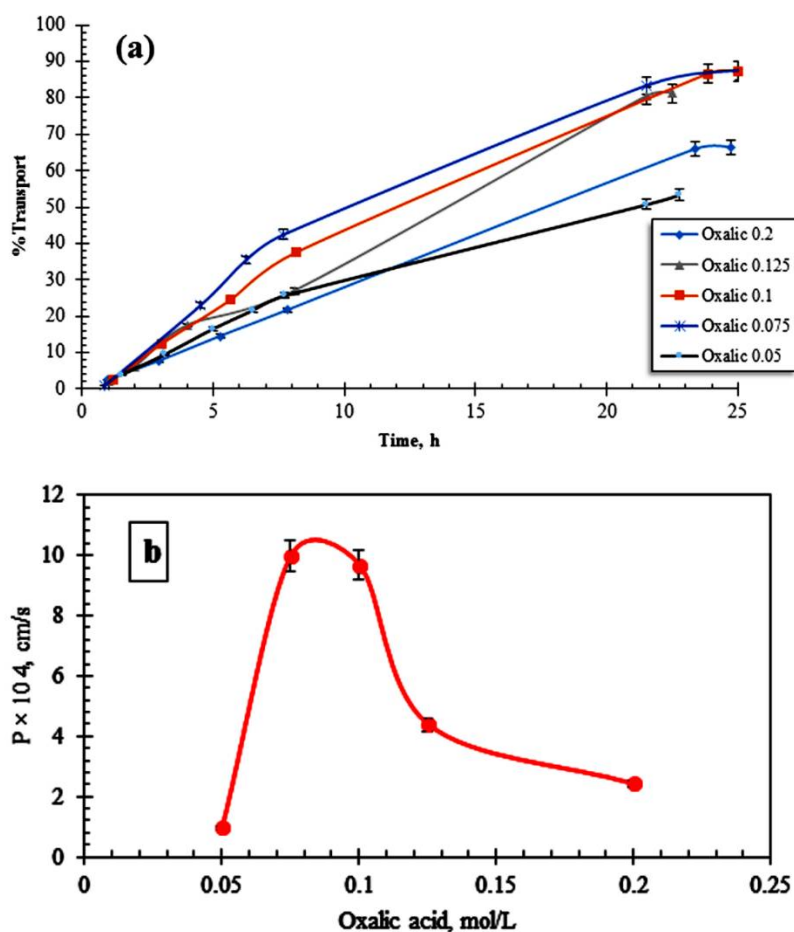


**Figure 1.** Liquid-liquid extraction: log D versus log [Cyanex 923] ([Ge(IV)] = 100 mg/L; [oxalic acid] = 0.1 mol/L).

### 158 4.2. Determination of appropriate concentrations for oxalic acid in the feed phase

159 With respect to the "solution chemistry" section, germanium was transported across FSSLM as  
160 a neutral complex (trisoalato germanate) using Cyanex 923. The transport depended on the degree  
161 of germanium complexation with oxalates. Therefore, the concentration of oxalic acid was a  
162 significant parameter for this transportation. In this regard, a series of experiments were conducted

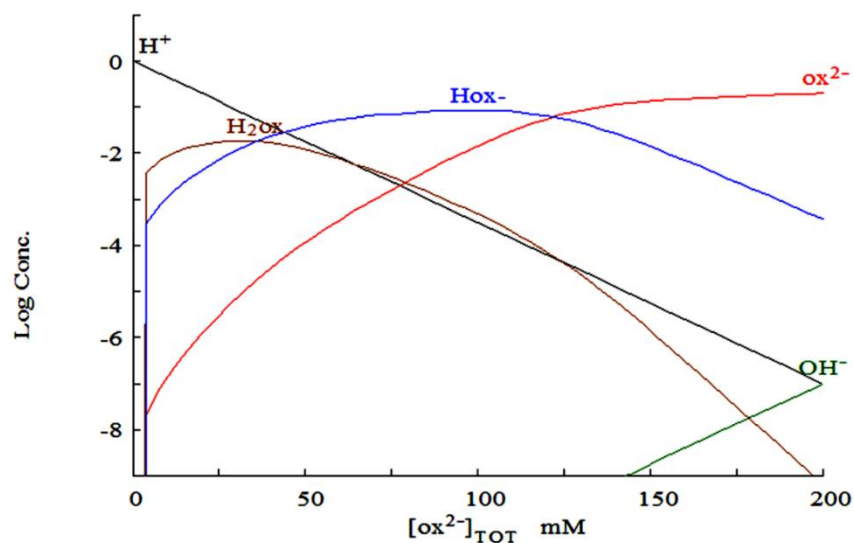
163 at the oxalic acid concentration in the range of 0.05-0.2 mol/L with the carrier concentration of 20  
 164 %v/v. The maximum transport has been achieved at the oxalic acid concentrations in the range of  
 165 0.075-0.1 mol/L with the transport efficiency of more than 88%. Figure 2a and b illustrates the  
 166 obtained results. As seen in this figure, the transport efficiency and permeation coefficients  
 167 descended at lower and higher than this range. The maximum permeation coefficient and transport  
 168 efficiency were found at the oxalic concentration of 0.075 to be  $9.97 \times 10^{-4}$  cm/s and 88%,  
 169 respectively. In order to know the reason for this behavior, the speciation diagram and the extraction  
 170 reaction of germanium by Cyanex 923 should be considered. As discussed in the previous section, to  
 171 transport germanium, 1 molecule of germanium-oxalate that joined 2 molecules of  $H^+$  was extracted  
 172 by 4 molecules of Cyanex 923. Therefore, to transport germanium species, the presence of  $H^+$  and  
 173 oxalate anions ( $ox^{2-}$ ) hydrolyzed from oxalic acid ( $H_2ox$ ) is vital. The speciation diagram of oxalic  
 174 acid has been illustrated in Figure 3. As seen in this figure, at lower oxalic acid concentration, the  
 175 dissociation of oxalic acid ( $H_2ox$ ) is not complete, whereas by increasing the oxalic acid  
 176 concentration, the concentration of  $ox^{2-}$  enhances. On the other hand, with increasing the total oxalic  
 177 acid concentration, the concentration of  $H^+$  decreases resulting in the decrease of the germanium  
 178 transport at higher oxalic acid concentration. Therefore, it can be concluded that the lack of oxalate  
 179 ( $ox^{2-}$ ) and  $H^+$  molecules descended the transport efficiency at the lower and higher oxalic acid  
 180 concentrations, respectively.



181

182

183 **Figure 2.** The effect of oxalic acid concentration on (a) the transport and (b) permeability coefficient  
 184 of germanium across the FSSLM system ([Cyanex 923] = 20 %v/v, the temperature of 22oC, and  
 185 [NaOH]= 0.1 mol/L).



186

187

**Figure 3.** Speciation diagram of oxalic acid calculated by Medusa software.

188

#### 4.3. Evaluation of appropriate carrier concentration

189

190

191

192

193

194

195

196

197

198

199

200

201

202

203

204

205

206

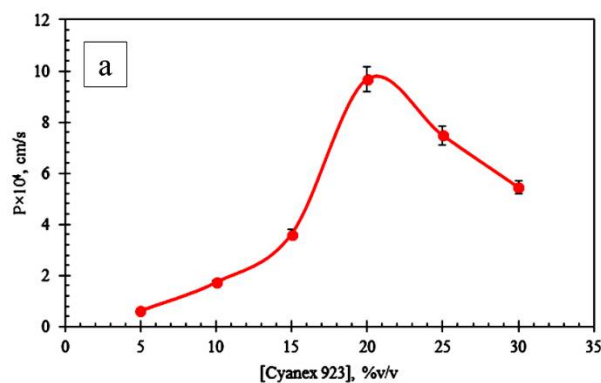
207

208

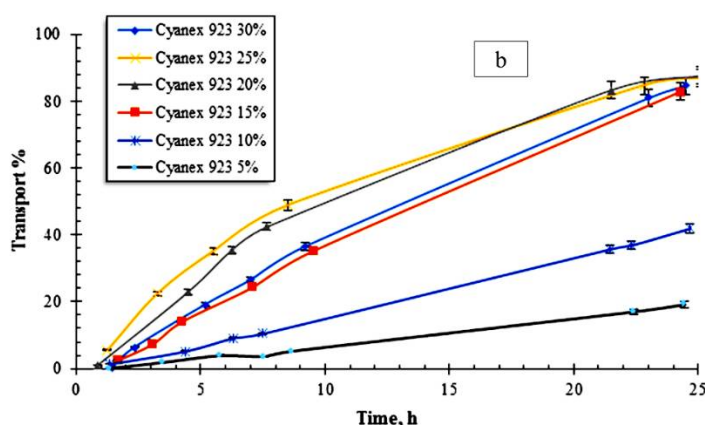
209

210

The presence of mobile carriers in the membrane phase is necessary for the transport phenomena, but an excess amount enhances the viscosity, decreasing transport [27]. Therefore, in order to obtain an appropriate transport, determining an optimum concentration of the carrier is important. According to the literature, the selection of a carrier concentration range for SLM experiments depends on the type of species and other factors. For instance, Rathore, Leopold, Pabby, Fortuny, Coll, and Sastre [18] investigated the effect of Cyanex 923 concentration as a carrier on the transport of Cd(II) across an SLM system in the range of 0 to 20 %v/v. Moreover, the Cyanex 923 concentration of 20-80 %v/v was applied to transport Cd(II) from a chloride medium via an FSSLM system [28]. In the present study, the range of 0-30 %v/v for the extractant concentration was selected with respect to the liquid-liquid extraction experiments. All FSSLM experiments were conducted at the oxalic acid concentration of 0.075 mol/L, the temperature of 22°C, and the NaOH concentration of 0.1 mol/L. The result has been plotted in Figure 4a and b. As seen in this figure, the germanium transport efficiency increased up to 88% when the carrier concentration of reached 20 %v/v. As seen in this figure, the complete reaction between species and the carrier does not occur at lower concentrations of the carrier. Moreover, with increasing the carrier concentration, the curve corresponding to Cyanex 923 of 30 and 25 %v/v was shifted down, showing the decrease of the germanium transport. In Figure 4b, this behavior can be observed in the reduction of the permeability coefficient. The reduction occurred due to the enhancement of Cyanex 923 viscosity and its precipitation in pores of the membrane [29]. According to the aforementioned discussion, the concentration of 20 %v/v was selected as an optimum concentration.



211

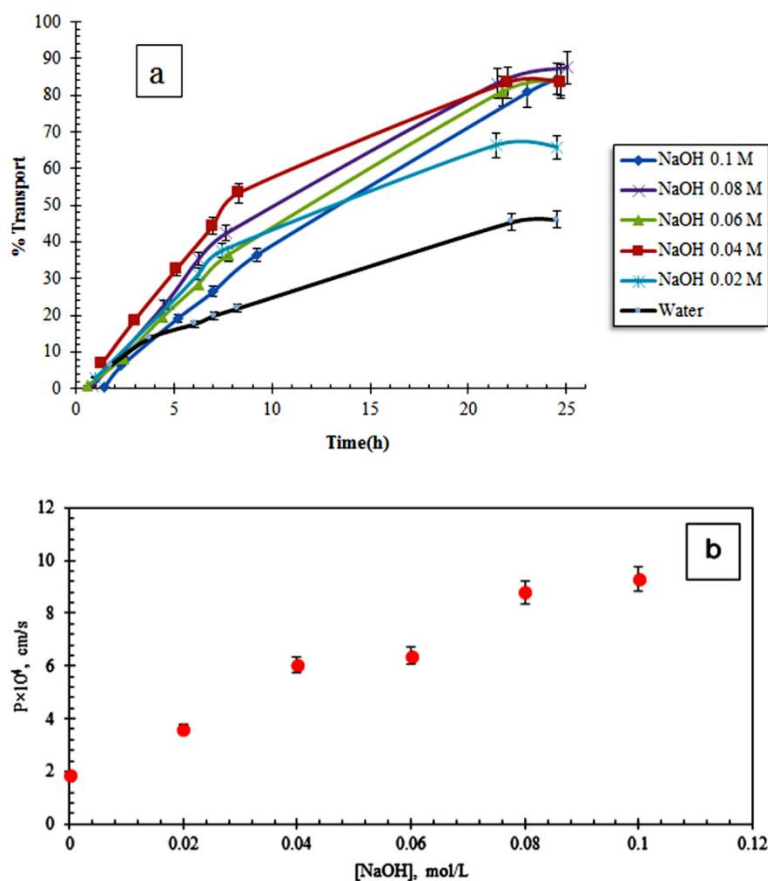


212

213 **Figure 4.** Effect of the carrier concentration on (a) the transport and (b) permeability coefficient of  
 214 germanium across the FSSLM system ( $[\text{Oxalic acid}] = 0.075 \text{ mol/L}$ , temperature of  $22^\circ\text{C}$ , and  $[\text{NaOH}]$   
 215  $= 0.1 \text{ mol/L}$ ).

#### 216 4.4. Investigation on appropriate strip reagent

217 In order to select efficient reagent/reagents for stripping germanium from the loaded organic  
 218 carrier, a series of liquid-liquid extraction experiments were conducted. In this regard, several  
 219 reagents, which were predicted to be efficient in the stripping process including ammonium chloride  
 220 ( $\text{NH}_4\text{Cl}$ ), sodium hydroxide ( $\text{NaOH}$ ), catechol ( $\text{C}_6\text{H}_6\text{O}_2$ ), citric acid ( $\text{C}_6\text{H}_8\text{O}_7$ ), ammonia ( $\text{NH}_3$ ),  
 221 sodium sulfate ( $\text{Na}_2\text{SO}_4$ ), and sulfuric acid ( $\text{H}_2\text{SO}_4$ ) were tested. The results have been published  
 222 elsewhere [30]. Based on the results,  $\text{NaOH}$  was selected as an efficient reagent for stripping  
 223 germanium from 20 %v/v Cyanex 923. Thus, FSSLM experiments were conducted to evaluate the  
 224 effect of the  $\text{NaOH}$  concentration on the transport of germanium with the carrier concentration of  
 225 Cyanex 923 20 %v/v in an oxalic acid concentration of 0.075 mol/L in the feed phase. The results can  
 226 be seen in Figure 5a and b.



227

228

229

230

231

**Figure 5.** Effect of NaOH concentration on (a) transport and (b) permeability coefficient of germanium stripped to the receiving phase across the FSSLM system ([Oxalic acid] = 0.075 mol/L, the temperature of 22oC, and [Cyanex 923] = 20 %v/v).

232

233

234

235

236

237

238

239

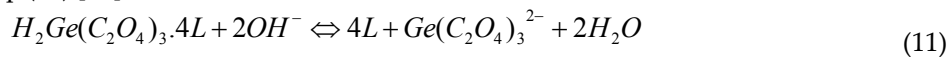
240

241

As seen in this figure, the transport efficiency and permeability coefficient increase with an enhancement of NaOH concentration, as at concentrations of more than 0.08 mol/L, >88% of germanium was transferred to the strip phase. The transport efficiencies corresponding to NaOH concentrations of 0.06 and 0.04 mol/L are approximately 84%. Furthermore, according to Figure 5b, the permeability coefficient increased up to  $9.20 \times 10^{-4}$  cm/s at the NaOH concentration of 0.1 mol/L. This is due to the increased amount of OH<sup>-</sup> anions, enhancing the de-complexation rate at the interface of the strip side [25].  $H_2Ge(C_2O_4)_3$  species are transported by Cyanex 923 from the feed solution followed by diffusing through the membrane phase and stripping in the interface of the receiving solution. The probable reaction for stripping species from the loaded carrier can be written as Eq. (11) [30]:

242

243



244

#### 4.5. Effect of membrane PVDF type on the transport

245

246

247

248

249

250

251

252

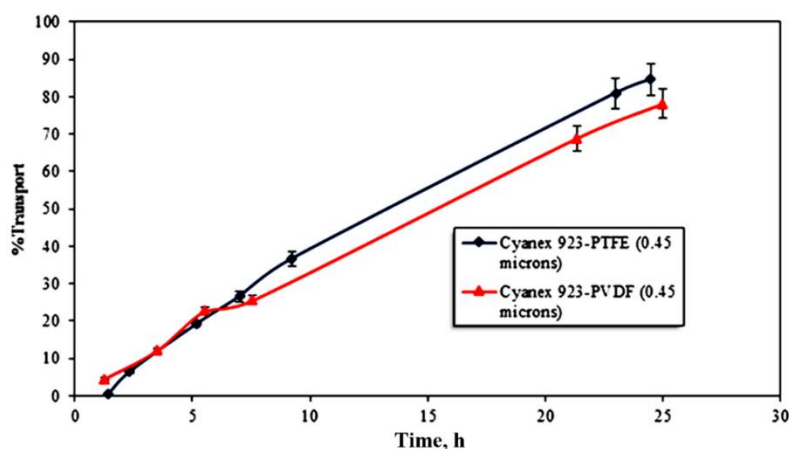
253

In order to know the transport behavior of germanium through a polyvinylidene difluoride (PVDF) membrane, a transport experiment was conducted the condition of 100 mg/L Ge, Ni, Cd, Co and 1000 mg/L of Zn; oxalic acid of 0.075 mol/L, and the NaOH concentration of 0.1 mol/L in the strip phase. The PVDF membrane used had a pore size of 0.45  $\mu$ m, the porosity of 80% and thickness of 125  $\mu$ m.

As seen in Figure 6, there is not a significant difference between the transport efficiencies corresponding to the PTFE and PVDF membranes obtained from the experiments conducted under a similar condition. However, the overall transport efficiency of the PTFE membrane is higher. The germanium permeability coefficients belonging to the PVDF and PTFE membranes were obtained to be  $3.14 \times 10^{-4}$  and  $9.28 \times 10^{-4}$  cm/s, respectively. Therefore, the germanium permeability through the



254 PTFE membrane is approximately 3 times the PVDF permeability. Similar results have been  
 255 reported by Adnan, *et al.* [31]. Various parameters such as higher tortuosity of PVDF membranes  
 256 and thickness are resulted in reducing their permeability [32].



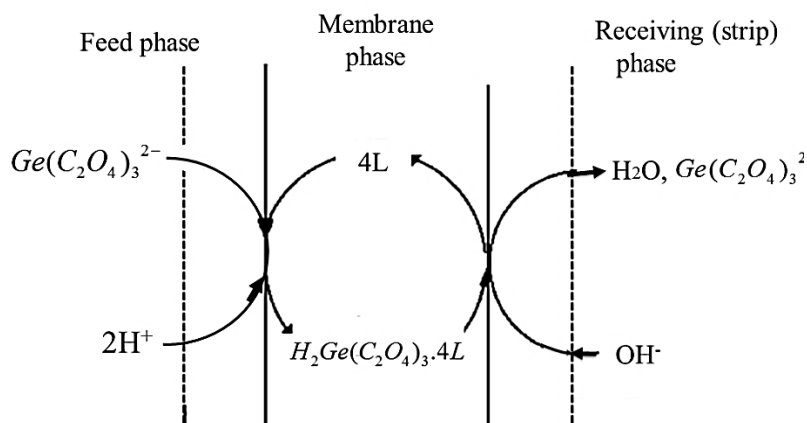
257

258 **Figure 6.** Transport efficiency of germanium versus time across PTFE and PVDF membranes (100  
 259 mg/L of Ge, Ni, Cd, Co and 1000 mg/L of Zn, the oxalic acid of 0.075 mol/L, and the NaOH  
 260 concentration of 0.1 mol/L in the strip phase).

#### 261 4.6. Permeability model

262 The permeation of Ge(IV) through the FSSLM (with PTFE membrane) of this study was  
 263 modeled to find mass transfer resistances. To model the mentioned system, it was assumed that the  
 264 species transport through SLM was performed by diffusing, and chemical reactions took place  
 265 promptly [33]. Figure 7 illustrates how germanium oxalates permeate through a PTFE membrane  
 266 containing Cyanex 923 based on the following steps:

- 267 (i) in the feed phase, the germanium oxalates and protons diffuse to the interface layer.  
 268 (ii) diffused species and the Cyanex 923 molecules react together at the mentioned layer.  
 269 (iii) the produced complexes permeate across the membrane toward the membrane-strip  
 270 interface layer.  
 271 (iv) NaOH detaches germanium-Cyanex 923 complexes at the membrane-strip phase interface.  
 272 Thus, germanium is stripped from the organic carrier.  
 273 (v) the unloaded carrier molecules permeate inversely toward the feed phase.



274

275 **Figure 7.** A schematic transport of germanium through FSSLM-Cyanex923.

276 The extraction equilibrium reaction of germanium by Cyanex 923 has been described in Eq. (8)  
 277 with  $n=4$ . According to the experimental data, the extraction equilibrium constant of this reaction  
 278 was calculated to be 2056. The germanium flux can be obtained using Fick's first diffusion law.

279 Hence, the fluxes at the feed-membrane boundary layer and the membrane phase ( $J_f$  and  $J_m$ ,  
280 respectively) can be provided as Eqs. (12) and (13):

$$281 \quad J_f = \frac{1}{\Delta_f} ([Ge(IV)]_f - [Ge(IV)]_{bl,f}) \quad (12)$$

$$282 \quad J_m = \frac{1}{\Delta_m} ([H_2Ge(ox)_3 \cdot 4R]_{bl,f} - [H_2Ge(ox)_3 \cdot 4R]_{bl,s}) \quad (13)$$

283 Where  $\Delta_m$  and  $\Delta_f$  depict the resistances corresponding to the membrane phase and the feed  
284 phase boundary layer, respectively. Subscripts of f, bl, and s show feed, boundary layer, and strip,  
285 respectively. Moreover,  $[Ge(IV)]_f$ ,  $[H_2Ge(ox)_3 \cdot 4R]_{bl,f}$  and  $[H_2Ge(ox)_3 \cdot 4R]_{bl,s}$  represent the  
286 germanium concentration in the feed phase, the feed-membrane boundary layer, and the  
287 strip-membrane boundary layer, respectively. It is noted that since the germanium concentration in  
288 the membrane-strip boundary layer is lower than that in the feed-membrane boundary layer, [  
289  $H_2Ge(ox)_3 \cdot 4R]_{bl,s}$  has been neglected. Hence, Eq. (13) can be rewritten as Eq. (14):

$$290 \quad J_m = \frac{1}{\Delta_m} ([H_2Ge(ox)_3 \cdot 4R]_{bl,f}) \quad (14)$$

291 Since chemical reactions promptly took place, the flux values in the feed-membrane layer and  
292 the membrane phase are equal ( $J_f = J_m = J$ ). Therefore, overall  $J$  can be found as Eq. (15):

$$293 \quad J = \frac{K[H^+]^2[R]_{org}^4[Ge(IV)]_f}{\Delta_m + \Delta_f(K[H^+]_{aq}^2[R]_{org}^4)} \quad (15)$$

295

296

297

298

299

300

301

302

303

304

305

306

307

308

309

310

311

312

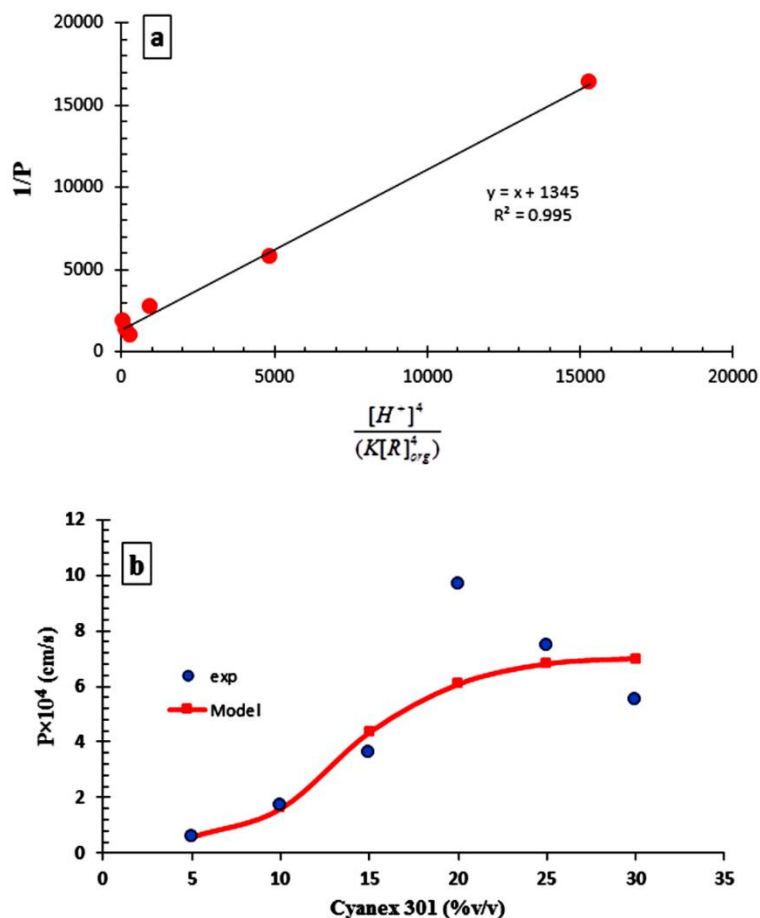
Regarding Eq. (1), the permeability coefficient is also written as Eq. (16):

$$299 \quad P = \frac{K[H^+]^2[R]_{org}^4}{\Delta_m + \Delta_f(K[H^+]_{aq}^2[R]_{org}^4)} \quad (16)$$

By arranging Eq. (16), Eq. (17) was found to obtain mass transfer resistances:

$$304 \quad \frac{1}{P} = \Delta_f + \frac{\Delta_m}{(K[H^+]_{aq}^2[R]_{org}^4)} \quad (17)$$

306 By plotting  $\frac{1}{(K[H^+]_{aq}^2[R]_{org}^4)}$  versus  $1/P$ , and the corresponding trend line, the intercept and the  
307 slope of the trend line can be found which are  $\Delta_f$  and  $\Delta_m$ , respectively. The mentioned plot was  
308 shown in Figure 8a. According to this plot, the values of 1 and 1345 s/cm were found for  $\Delta_m$  and  $\Delta_f$ ,  
309 respectively. Also, the permeation coefficient was found according to Eq. (16). The plot of calculated  
310  $P$  ( $P_{cal}$ ) and experimental  $P$  ( $P_{exp}$ ) as a function of the Cyanex 923 concentration was constructed as  
311 Figure 8b. As seen in this figure, the  $P_{exp}$  value increased up to the concentration of 20 %v/v  
312 followed by a decrease due to the enhancement of viscosity. On the other hand, the model points  
313 constructed a curve showing the trend of the permeation enhancement. However, a sudden up and  
314 down at the carrier concentration of 20 %v/v, could not be calculated by the model. The model curve  
315 showed the regular trend of the permeation, as the  $P$  value increased with an enhancement of the  
316 carrier concentration up to 20 %v/v, but above this concentration, the value reached a plateau  
317 because the viscosity governed the transport process.



318

319

320

321

322

323

## 5. Conclusion

324

325

326

327

328

329

330

331

332

333

334

335

336

337

338

339

340

Figure 8. (a) The plot of  $1/P$  vs.  $\frac{[H^+]^4}{(K[R]_{org}^4)}$  (b) Effect of the concentration of Cyanex 301 as a carrier in the SLM system on the germanium permeability coefficient (Aqueous feed phase: pH= 1.5; Stripping phase:  $[H_2SO_4]= 400$  g/dm<sup>3</sup>; and contact time= 20).

In this study, the transport of germanium was investigated across an FSSLM system from aqueous solutions. The main achievement of this study was that germanium oxalate neutral species were effective through an FSSLM system containing Cyanex 923. The oxalic acid concentration is one of the parameters having a vital effect on the transport. As a result, an optimum concentration of oxalic acid for the complete transport of germanium was found at a concentration range of 0.075-0.1 mol/L. The investigation on the effect of the Cyanex 923 concentration in the membrane phase showed that the concentration of 20 %v/v was appropriate for the complete germanium transportation. Several stripping reagents were classified based on liquid-liquid extraction experiments to select appropriate reagents used in the FSSLM system. Accordingly, NaOH was chosen as an efficient stripping reagent for the FSSLM system. In the FSSLM experiments with higher concentrations of NaOH in the strip phase, the higher germanium transport was observed. The NaOH concentration range of 1-3 mol/dm<sup>3</sup> was obtained in this process. The permeation model was developed to find the mass transfer resistances. As a result, the values of 1 and 1345 s/cm were found for  $\Delta m$  and  $\Delta f$ , respectively. The model curve showed the regular trend of the permeation, as the  $P$  value reached a plateau at higher carrier concentrations because the viscosity governed the transport process.

## 341 Acknowledgments

342 This study was carried out in the Department of Chemical Engineering, Universitat Politècnica  
343 de Catalunya, Vilanova i la Geltrú Campus, Spain. The authors wish to acknowledge Dr. Agustín  
344 Fortuny and Dr. Maria Teresa Coll for their assistance and scientific consultation.

345 **Author Contributions:** H.K.H made a significant contribution to every stage of this paper, such as the  
346 investigation (with the essential assistance of A.M.S) and analysis and preparing the paper. M.I. contributed to  
347 the conception of the paper. H.K.H designed the tests and presented a model for this paper. M.I. and H.K.H  
348 finalized the paper by a critical revision of the paper.

349 **Acknowledgments:** This research was implemented in the Department of Chemical Engineering, Universitat  
350 Politècnica de Catalunya (Barcelona-Tec), Spain. The authors acknowledge Dr. Agustín Fortuny for his help.

## 351 References

- 352 1. Liu, F.; Liu, Z.; Li, Y.; Wilson, B.P.; Lundström, M. Recovery and separation of gallium(III) and  
353 germanium(IV) from zinc refinery residues: Part I: Leaching and iron(III) removal. *Hydrometallurgy*  
354 **2017**, *169*, 564-570, doi:<https://doi.org/10.1016/j.hydromet.2017.03.006>.
- 355 2. Liu, F.; Liu, Z.; Li, Y.; Wilson, B.P.; Lundström, M. Recovery and separation of gallium(III) and  
356 germanium(IV) from zinc refinery residues: Part I: Leaching and iron(III) removal. *Hydrometallurgy*  
357 **2017**, doi:<http://dx.doi.org/10.1016/j.hydromet.2017.03.006>.
- 358 3. Zhang, L.; Xu, Z. Application of vacuum reduction and chlorinated distillation to enrich and prepare  
359 pure germanium from coal fly ash. *Journal of Hazardous Materials* **2017**, *321*, 18-27,  
360 doi:<http://dx.doi.org/10.1016/j.jhazmat.2016.08.070>.
- 361 4. Makowska, D.; Wieróńska, F.; Strugała, A.; Kosowska, K. Germanium content in Polish hard coals. In  
362 Proceedings of E3S Web of Conferences; p. 00121.
- 363 5. Liu, F.; Liu, Z.; Li, Y.; Liu, Z.; Li, Q.; Zeng, L. Extraction of gallium and germanium from zinc refinery  
364 residues by pressure acid leaching. *Hydrometallurgy* **2016**, *164*, 313-320,  
365 doi:<https://doi.org/10.1016/j.hydromet.2016.06.006>.
- 366 6. Torralvo, F.A.; Fernández-Pereira, C. Recovery of germanium from real fly ash leachates by  
367 ion-exchange extraction. *Miner. Eng.* **2011**, *24*, 35-41, doi:<https://doi.org/10.1016/j.mineng.2010.09.004>.
- 368 7. Arroyo, F.; Font, O.; Fernández-Pereira, C.; Querol, X.; Juan, R.; Ruiz, C.; Coca, P. Germanium recovery  
369 from gasification fly ash: Evaluation of end-products obtained by precipitation methods. *Journal of*  
370 *Hazardous Materials* **2009**, *167*, 582-588, doi:<http://dx.doi.org/10.1016/j.jhazmat.2009.01.021>.
- 371 8. Hernández-Expósito, A.; Chimenos, J.; Fernández, A.; Font, O.; Querol, X.; Coca, P.; Peña, F.G. Ion  
372 flotation of germanium from fly ash aqueous leachates. *Chem. Eng. J.* **2006**, *118*, 69-75.
- 373 9. Kuroiwa, K.; Ohura, S.-i.; Morisada, S.; Ohto, K.; Kawakita, H.; Matsuo, Y.; Fukuda, D. Recovery of  
374 germanium from waste solar panels using ion-exchange membrane and solvent extraction. *Miner. Eng.*  
375 **2014**, *55*, 181-185.
- 376 10. Cui, W.; Wang, S.; Peng, J.; Zhang, L.; Zhang, G. Catechol-functionalized nanosilica for adsorption of  
377 germanium ions from aqueous media. *Journal of Sol-Gel Science and Technology* **2016**, *77*, 666-674.
- 378 11. Arroyo, F.; Fernández-Pereira, C.; Bermejo, P. Demonstration Plant Equipment Design and Scale-Up  
379 from Pilot Plant of a Leaching and Solvent Extraction Process. *Minerals* **2015**, *5*, 298-313.
- 380 12. Arroyo, F.; Fernández-Pereira, C. Hydrometallurgical Recovery of Germanium from Coal Gasification  
381 Fly Ash. Solvent Extraction Method. *Industrial & Engineering Chemistry Research* **2008**, *47*, 3186-3191,  
382 doi:10.1021/ie7016948.
- 383 13. Leepipatpiboon, N.; Pancharoen, U.; Ramakul, P. Separation of Co(II) and Ni(II) from thiocyanate  
384 media by hollow fiber supported liquid membrane containing Alamine300 as carrier — investigation

- 385 on polarity of diluent and membrane stability. *Korean Journal of Chemical Engineering* **2013**, *30*, 194-200,  
386 doi:10.1007/s11814-012-0111-3.
- 387 14. Ruhela, R.; Panja, S.; Sharma, J.N.; Tomar, B.S.; Tripathi, S.C.; Hubli, R.C.; Suri, A.K. Facilitated  
388 transport of Pd(II) through a supported liquid membrane (SLM) containing  
389 N,N,N',N'-tetra-(2-ethylhexyl) thiodiglycolamide T(2EH)TDGA: A novel carrier. *J. Hazard. Mater.* **2012**,  
390 229-230, 66-71, doi:<https://doi.org/10.1016/j.jhazmat.2012.05.064>.
- 391 15. Kamran Haghghi, H.; Irannajad, M.; Moradkhani, D. Permeation and modeling studies on Ge(IV)  
392 facilitated transport using TOA through supported liquid membrane. *Korean Journal of Chemical*  
393 *Engineering* **2017**, *Accepted Article*.
- 394 16. Prakorn, R.; Eakkapit, S.; Weerawat, P.; Milan, H.; Ura, P. Permeation study on the hollow-fiber  
395 supported liquid membrane for the extraction of Cobalt(II). *Korean Journal of Chemical Engineering* **2006**,  
396 23, 117-123, doi:10.1007/BF02705702.
- 397 17. Zaheri, P.; Abolghasemi, H.; Mohammadi, T.; Maraghe, M.G. Synergistic extraction and separation of  
398 Dysprosium and Europium by supported liquid membrane. *Korean Journal of Chemical Engineering*  
399 **2015**, *32*, 1642-1648, doi:10.1007/s11814-014-0350-6.
- 400 18. Rathore, N.S.; Leopold, A.; Pabby, A.K.; Fortuny, A.; Coll, M.T.; Sastre, A.M. Extraction and  
401 permeation studies of Cd(II) in acidic and neutral chloride media using Cyanex 923 on supported  
402 liquid membrane. *Hydrometallurgy* **2009**, *96*, 81-87,  
403 doi:<http://dx.doi.org/10.1016/j.hydromet.2008.08.009>.
- 404 19. Alguacil, F.J.; López-Delgado, A.; Alonso, M.; Sastre, A.M.a. The phosphine oxides Cyanex 921 and  
405 Cyanex 923 as carriers for facilitated transport of chromium (VI)-chloride aqueous solutions.  
406 *Chemosphere* **2004**, *57*, 813-819, doi:<http://dx.doi.org/10.1016/j.chemosphere.2004.07.019>.
- 407 20. Alguacil, F.J.; Martínez, S. Solvent extraction of Zn (II) by Cyanex 923 and its application to a solid-  
408 supported liquid membrane system. *Journal of chemical technology and biotechnology* **2001**, *76*, 298-302.
- 409 21. Alguacil, F.J.; Martínez, S. Permeation of iron(III) by an immobilised liquid membrane using Cyanex  
410 923 as mobile carrier. *Journal of Membrane Science* **2000**, *176*, 249-255,  
411 doi:[http://dx.doi.org/10.1016/S0376-7388\(00\)00442-7](http://dx.doi.org/10.1016/S0376-7388(00)00442-7).
- 412 22. Alguacil, F.J.; Coedo, A.G.; Dorado, M.T.; Padilla, I. Phosphine oxide mediate transport: modelling of  
413 mass transfer in supported liquid membrane transport of gold (III) using Cyanex 923. *Chem. Eng. Sci.*  
414 **2001**, *56*, 3115-3122, doi:[https://doi.org/10.1016/S0009-2509\(01\)00014-8](https://doi.org/10.1016/S0009-2509(01)00014-8).
- 415 23. Singh, S.K.; Misra, S.K.; Tripathi, S.C.; Singh, D.K. Studies on permeation of uranium (VI) from  
416 phosphoric acid medium through supported liquid membrane comprising a binary mixture of PC88A  
417 and Cyanex 923 in n-dodecane as carrier. *Desalination* **2010**, *250*, 19-25,  
418 doi:<http://dx.doi.org/10.1016/j.desal.2009.06.067>.
- 419 24. Rathore, N.S.; Leopold, A.; Pabby, A.K.; Fortuny, A.; Coll, M.T.; Sastre, A.M. Extraction and  
420 permeation studies of Cd(II) in acidic and neutral chloride media using Cyanex 923 on supported  
421 liquid membrane. *Hydrometallurgy* **2009**, *96*, 81-87,  
422 doi:<http://dx.doi.org/10.1016/j.hydromet.2008.08.009>.
- 423 25. Arslan, G.; Tor, A.; Muslu, H.; Ozmen, M.; Akin, I.; Cengeloglu, Y.; Ersoz, M. Facilitated transport of  
424 Cr(VI) through a novel activated composite membrane containing Cyanex 923 as a carrier. *Journal of*  
425 *Membrane Science* **2009**, *337*, 224-231, doi:<https://doi.org/10.1016/j.memsci.2009.03.049>.

- 426 26. Nosrati, S.; Jayakumar, N.S.; Hashim, M.A. Extraction performance of chromium (VI) with emulsion  
427 liquid membrane by Cyanex 923 as carrier using response surface methodology. *Desalination* **2011**, *266*,  
428 286-290, doi:<http://dx.doi.org/10.1016/j.desal.2010.08.023>.
- 429 27. Bhatluri, K.K.; Manna, M.S.; Ghoshal, A.K.; Saha, P. Supported liquid membrane based removal of  
430 lead (II) and cadmium (II) from mixed feed: Conversion to solid waste by precipitation. *Journal of*  
431 *hazardous materials* **2015**, *299*, 504-512.
- 432 28. Alguacil, F.J.; Tayibi, H. Carrier-facilitated transport of Cd(II) from a high-salinity chloride medium  
433 across a supported liquid membrane containing Cyanex 923 in Solvesso 100. *Desalination* **2005**, *180*,  
434 181-187, doi:<http://dx.doi.org/10.1016/j.desal.2004.12.036>.
- 435 29. Przewoźna, M.; Gajewski, P.; Michalak, N.; Bogacki, M.B.; Skrzypczak, A. Determination of the  
436 Percolation Threshold for the Oxalic, Tartaric, and Lactic Acids Transport through Polymer Inclusion  
437 Membranes with 1-Alkylimidazoles as a Carrier. *Sep. Sci. Technol.* **2014**, *49*, 1745-1755,  
438 doi:10.1080/01496395.2014.906464.
- 439 30. Kamran Haghighi, H.; Irannajad, M.; Fortuny, A.; Sastre, A.M. Recovery of germanium from leach  
440 solutions of fly ash using solvent extraction with various extractants. *Hydrometallurgy* **2018**, *175*,  
441 164-169, doi:<https://doi.org/10.1016/j.hydromet.2017.11.006>.
- 442 31. Adnan, S.; Hoang, M.; Wang, H.; Xie, Z. Commercial PTFE membranes for membrane distillation  
443 application: effect of microstructure and support material. *Desalination* **2012**, *284*, 297-308.
- 444 32. Zhang, J.; Duke, M.; Ostarcevic, E.; Dow, N.; Gray, S.; Li, J.-d. Performance of new generation  
445 membrane distillation membranes. *Water Science and Technology: Water Supply* **2009**, *9*, 501.
- 446 33. Alonso, M.; López-Delgado, A.; Sastre, A.M.; Alguacil, F.J. Kinetic modelling of the facilitated  
447 transport of cadmium (II) using Cyanex 923 as ionophore. *Chem. Eng. J.* **2006**, *118*, 213-219,  
448 doi:<https://doi.org/10.1016/j.cej.2006.02.006>.
- 449
- 450